Fitoterapia 137 (2019) 104194

Contents lists available at ScienceDirect

Fitoterapia

journal homepage: www.elsevier.com/locate/fitote

Dimeric tetrahydroxanthones from the lichen *Usnea aciculifera*

Truong L. Tuong[a], Thammarat Aree[a], Lien T.M. Do[b], Phung K.P. Nguyen[c], Piyanuch Wonganan[d], Warinthorn Chavasiri[a,*]

[a] Center of Excellence in Natural Products Chemistry, Department of Chemistry, Faculty of Science, Chulalongkorn University, Phayathai Road, Patumwan, Bangkok 10330, Thailand
[b] Institute of Environment-Energy Technology, Sai Gon University, Ho Chi Minh City 748355, Viet Nam
[c] University of Science, National University–Ho Chi Minh City, Ho Chi Minh City 748355, Viet Nam
[d] Department of Pharmacology, Faculty of Medicine, Chulalongkorn University, Bangkok 10330, Thailand

ARTICLE INFO

Keywords:
Usnea aciculifera
Dimeric xanthones
Tetrahydroxanthone
Usneaxanthones A–D
Cytotoxicity

ABSTRACT

Four unusual heterodimeric tetrahydroxanthones, usneaxanthones A–D (**1**–**4**) were isolated from lichen *Usnea aciculifera* Vain (Parmeliaceae). Their structures and absolute configurations, particularly the central and axial chiralities, were unambiguously demonstrated by a combination of spectroscopic data (1D, 2D NMR, HRESIMS), electronic circular dichroism (ECD) experiments, and single-crystal X-ray crystallographic analyses. Cytotoxic effects of isolated compounds (**1**, **2** and **4**) were evaluated on HT–29 human colorectal cancer cells. Compound **4** showed potent cytotoxicity against HT–29 with IC_{50} values of 2.41 μM.

1. Introduction

Xanthone dimers are widespread, structurally-diverse family of natural products and frequently found in plants, fungi and lichens. They feature an intriguing variety of linkages between the component xanthones. These synthetically elusive secondary metabolites are of great interest due to their broad array of bioactivities making xanthones being designated as “privileged structures”[1].

Dimeric tetrahydroxanthones and their derivatives like xanthone – chromanone and chromanone dimers, with attractive antibacterial [2,3], antifungal [4], and antimalarial activites [5], are a class of structurally interesting natural products produced by multiple fungal and lichenous species [6]. Several compounds with 2,2′-, 4,4′- or 4,2′-axial linkages have been isolated and identified since 1958 [6]. Biogenetically, most dimers are formed by two units from the same path [7], the biaryl bond is most often arranged in a 2,2′-manner with respect the common xanthone hydroxyl moiety such as the secalonic acids [1]. However, two path derived heterodimers with 4,2′- biaryl linkage are rare and only some molecules have been reported, such as namely eumitrins A1, A2, B, neosartorin, isoergochrysin, and lentulins A–H [8,9,10]. Although many dimeric xanthones, particularly the widespread secalonic acids, have been studied for many years [11], key aspects of their biosynthesis such as the mechanisms and timing of the dimerization process, and isolation and analysis of their biosynthetic gene clusters remain largely unknown. As Bringmann and co-workers noted in their seminal work on natural biaryl linkages “wherever in Nature phenolic aromatics can be found, the corresponding homo- or hetero-dimeric biaryls have to be expected” [12], the dimerization of xanthones remained a tricky subject for both the synthetic and biosynthetic chemist – the extent of the involvement of enzymes, and their nature, is at present unclear. There has been, at the time of writing, no direct observation of enzymatic dimerization of the monomer units.

All the dimeric tetrahydroxanthone analogues structurally involve axial chiral issues, which are different from the classic central chiralities, are interesting phenomena associated with the hindered rotation of a single bond [13]. Due to the multiple chirality centers, different monomeric units, and sometimes additional axial chirality elements, the determination of the relative and absolute configurations of the heterodimeric dimers are still challenging [2,5,14,15]. ECD calculation of the corresponding monomers combined with biogenetic considerations was commonly used method. However, the current approaches are ambiguous and lack efficiency, especially when (1) the ECD curves are dominated by the exciton coupled interaction of the two aryl moieties in axially chiral biaryl dimers, (2) they lack dominant conformations to calculate the time-dependent density functional theory (TDDFT)-ECD curves, especially for dimers with flexible moieties [16], 3) the tetrahydroxanthone or chromanone monomers and their corresponding dimers were often not co-isolated.

* Corresponding author at: Center of Excellence in Natural Products Chemistry, Department of Chemistry, Faculty of Science, Chulalongkorn University, 254 Phayathai Road, Patumwan District, Bangkok City, Thailand.
E-mail address: warinthorn.c@chula.ac.th (W. Chavasiri).

https://doi.org/10.1016/j.fitote.2019.104194
Received 2 May 2019; Received in revised form 2 June 2019; Accepted 4 June 2019
Available online 05 June 2019
0367-326X/

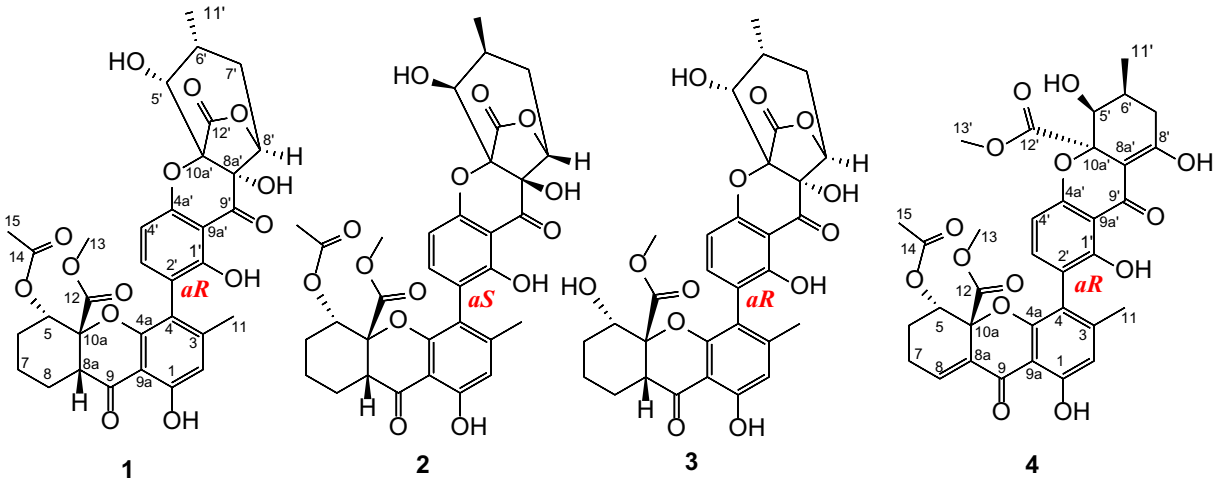

Fig. 1. Structures of compounds **1–4.**

During our search for bioactive constituents from the secondary metabolites of lichen *U. aciculifera*, four unusual heterodimeric tetrahydroxanthone, usneaxanthones A–D (**1–4**), were isolated. The absolute configurations of **1–4**, implying the central and axial chiral elements or preferred helicities, were established by a combination of X-ray diffraction analysis and ECD measurements. In addition, **4** exhibited potent cytotoxic activity against HT-29 human colorectal cancer cells. Herein, we report the fractionation of the CH_2Cl_2 extract leading to the isolation and structural determination (including relative and absolute configuration), and cytotoxic activity of these compounds.

2. Results and discussion

Usnea aciculifera thalii were collected in the Lam Dong province, Central Vietnam. Chromatographic fractionation of the CH_2Cl_2 extract led to the isolation of four new dimeric xanthones, named usneaxanthones **A–D** (**1–4**) (Fig. 1).

Usneaxanthone A (**1**), light yellow crystals, had a molecular formula of $C_{33}H_{32}O_{14}$ as determined by the HRESIMS through the protonated molecular ion at *m/z* 653.1862 $[M + H]^+$ (calcd for $C_{33}H_{32}O_{14}$ 653.1870) and the sodium adduct ion at *m/z* 675.1681 ($[M + Na]^+$, calcd 675.1645) (Fig. S6). The spectroscopic data, along with the consideration of the chemical profile of the genus *Usnea*, prompted us to speculate that **1** is an unsymmetrical dimeric tetrahydroxanthone. A combination of 2D NMR experiments and based on an AB coupling of the two proton substituents of each of these rings determined that the linkage between the two aryl positions must be 4,2′ – linkage.

The ^{1}H NMR spectrum of **1** showed the presence of two phenolic hydroxyl protons at δ_H 11.45 (1H, s) and 11.74 (1H, s), three aromatic protons at δ_H 6.46 (1H, s), δ_H 6.66 (1H, d, J = 8.4 Hz), and at 7.72 (1H, d, J = 8.4 Hz) (Table 1).

A careful analysis of its 1D and 2D NMR indicated that two partial structures **1a** and **1b** existed in **1** (Fig. 2) highly resembled that of eumitrin B [8]. However, detailed analysis revealed that the methoxycarbonyl group in the partial **1b** in eumitrin B was replaced by a γ-butyrolactone ring in **1** and the double bond conjugating to the ketone group in eumitrin B was transformed into a single bond with a hydroxyl group bonded to C-8'a in **1** instead of C-8′ in eumitrin B. The ^{1}H—^{1}H COSY correlations of H-5'/H-6'/H-7'/H-8′ and H-11′ (Fig. 2), along with the network of HMBC cross – peaks (Fig. 2) of H-5'/C-6′, C-10'a, C-12′; H-8'/C-9′, C-7′; H-11'/C-6′, C-7′, and C-8′, indicated the presence of a γ-butyrolactone ring, consisting of C-8'–C-8'a–C-10'a in **1** with a methyl (C-11′), and two hydroxyl groups at C-5′ and C-8'a, respectively. Thus, the planar structure of **1** was determined.

The relative configurations of **1** were determined by analysis of 1D and 2D NMR data, especially by coupling constants and experimental ECD spectrum of **1**. In the partial **1a**, the large coupling constants between proton H-5 and H-6 ($^3J_{5\text{-}6ax}$ = 11.2 Hz; $^3J_{5\text{-}6eq}$ = 4.8 Hz) and between H-8a and H-8 ($^3J_{8a\text{-}8ax}$ = 11.6 Hz; $^3J_{8a\text{-}8eq}$ = 4.0 Hz) suggested H-5 and H-8a were in the axial positions and the equatorial orientation for acetoxy group at C-5 and methoxycarbonyl at C-10a. For the partial **1b**, the small coupling constants between H-5′ and H-6′ ($^3J_{H\text{-}5'\text{-}H\text{-}6'}$ = 3.6 Hz), and H-8′ and H-7′ ($^3J_{H\text{-}8'\text{-}H\text{-}7'}$ = 3.6 Hz) suggested H-5′ and H-8′ must have an equatorial position. Finally, the assigned structure of **1** was unambiguously determined by using single-crystal X-ray diffraction analysis with Cu Kα radiation (Fig. 2). This analysis also enabled unambiguous assignment of the absolute configurations of the stereocenters in **1** as (5*S*,8a*S*,10a*R*,5′*R*, 6′*R*,8′*S*,8'a*S*).

The molecular formula $C_{33}H_{32}O_{14}$ of **2** was determined to be

Table 1
^{1}H NMR Spectroscopic Data for **1–4** (400 MHz, $CDCl_3$, δ ppm, J in Hz).

Position	1	2	3	4
2	6.46 s	6.49 s	6.52 s	6.49 s
5	4.97 dd (4.8,11.2)	4.98 dd (4.4, 10.8)	3.80 dd (4.4, 10.0)	5.43 dd (2.8, 4.4)
6	1.74 m	1.88 m	1.44 m 1.84 m	1.91 m 2.00 m
7	1.47 m	1.51 m	1.44 m	2.40 dd (11.2, 19.2)
	1.84 m	1.88 m	1.84 m	2.50 dd (6.0, 19.2)
8	1.47 m 1.84 m	1.51 m 1.84 m	1.44 m 1.84 m	7.30 m
8a	2.94 dd (4.0, 11.6)	3.00 d (4.8, 12.0)	2.92 dd (4.4, 12.0)	–
11	2.10 s	2.15 s	2.16 s	2.08 s
13	3.62 s	3.54 s	3.74 s	3.70 s
15	1.90 s	1.70 s	–	1.81 s
1-OH	11.45 s	11.44 s	11.54 s	12.01 s
3′	7.72 d (8.4)	7.40 d (8.0)	7.86 d (8.8)	7.26 d (8.0)
4′	6.66 d (8.4)	6.73 d (8.0)	6.80 d (8.8)	6.61 d (8.0)
5′	5.25 d (3.6)	5.30 d (3.6)	5.29 d (4.4)	4.17 brs
6′	2.14 m	2.21 m	2.20 m	2.12 m
7′	2.13 m	2.09 m	2.10 m	2.40 dd (11.2, 19.2)
	2.15 m	2.21 m		2.50 dd (6.0, 19.2)
8′	4.31 d (3.6)	4.40 d (2.8)	4.41 d (3.2)	–
11′	1.15 d (6.0)	1.21 d (5.2)	1.19 d (6.4)	1.18 d (6.4)
13′	–	–	–	3.77 s
1′-OH	11.74 s	11.71 s	11.76 s	11.59 s
5′-OH	–	–	6.55 s	–
8′-OH				13.93 s

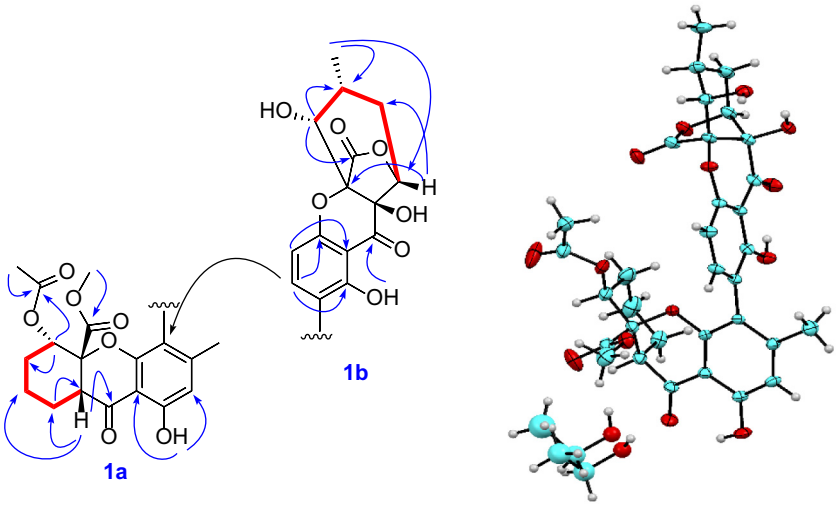

Fig. 2. Key 2D NMR correlations and X-ray structure of **1**.

identical to that of **1** by HRESIMS but showed different rotation value ($[\alpha]_D^{25}$ = −232 for **1** and + 286 for **2**).

The similarity of the ^{1}H and ^{13}C NMR resonances for **2** with those of **1** indicated that compound **2** has the same planar structure with those of **1**. The relative configurations in the monomeric unit **2a** of **2** was proposed to be the same as **1a**. However the small difference in the second monomeric unit **2b** was that the chemical shift of H-3′ upfield shifted from δ_H 7.72 in **1** to δ_H 7.40 in **2** (Table 1) suggested that the relative configurations in the partial **2b**, implying the central and axial chirality elements or preferred helicities of **2** will be differed with those of **1**. The axial chiralities were deduced on the basis of an ECD exciton chirality method [10]. The anticlockwise manner of the two benzoyl chromophores in **2** resulted in negative exciton couplings near 218 nm, allowing assignment of axial chirality as *aS* (Fig. 3) [10]. In contrast, the axial chirality in **1** was assigned to *aR* by positive exciton coupling near 213 nm (Fig. 3).

Furthermore, when a biaryl natural product contains both axial and central chirality elements, the ECD method can afford only the assignment of the axial chirality, as the ECD curves of axially chiral biaryl dimers generally dominated by the exciton coupled interaction of the two aryl moieties, which is governed by the sign and value of the biaryl torsional angle [17]. It is usually impracticable to determine the absolute configurations of the chirality centers by using the ECD method [18]. Therefore, with the aid of the single crystals, the absolute

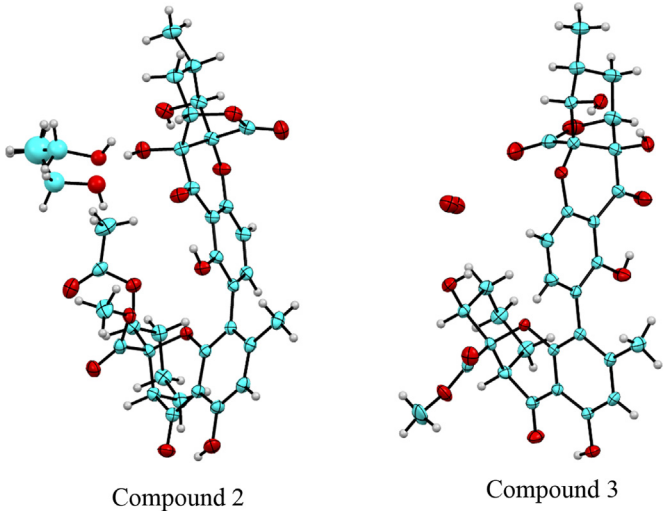

Fig. 4. ORTEP diagram of (**2**) and (**3**).

configurations of **2** were directly determined as (5*S*,8a*S*,10a*R*,5′*S*,6′*S*,8′*R*,8′a*R*) by X-ray diffraction analysis with Cu K*α* radiation [Flack parameter = 0.05 (9) (Fig. 4 and Table S1) [19].

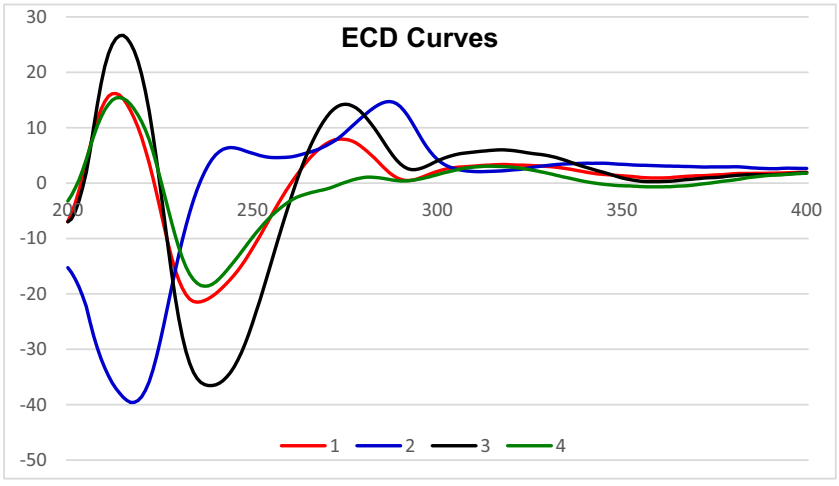

Fig. 3. Experimental ECD spectra of **1**–**4**.

Table 2
^{13}C NMR Spectroscopic Data for **1–4** (100 MHz, $CDCl_3$, δ ppm).

Position	1	2	3	4
1	161.5	161.8	162.0	162.1
2	111.2	111.2	111.6	111.2
3	150.8	150.9	150.9	150.4
4	115.4	115.6	114.9	115.7
4a	156.6	156.5	156.2	156.1
5	72.6	72.5	72.8	66.1
6	26.1	26.5	29.8	23.3
7	25.4	25.4	25.6	21.8
8	22.2	22.2	22.6	141.6
8a	48.6	48.5	48.9	128.9
9	197.7	197.6	197.8	184.7
9a	104.7	104.7	105.0	105.6
10a	83.3	83.3	85.2	80.9
11	21.2	21.3	21.3	21.1
12	169.7	169.7	170.6	169.0
13	53.3	53.3	53.3	53.5
14	170.7	170.3	–	169.7
15	20.6	20.5	–	20.3
1′	160.6	161.0	160.6	159.4
2′	117.6	118.1	117.6	117.6
3′	143.6	143.0	143.3	140.1
4′	107.0	107.2	107.8	107.9
4a'	158.1	157.8	158.3	157.3
5′	77.0	77.0	76.1	71.4
6′	29.5	29.4	29.5	28.5
7′	27.5	27.5	27.5	32.6
8′	74.3	74.8	74.5	179.6
8a'	76.0	76.0	77.0	100.2
9′	191.9	191.5	191.9	187.9
9a'	106.6	106.6	106.9	107.0
10a'	82.5	82.5	82.8	84.9
11′	15.3	15.4	15.4	17.5
12′	169.8	169.8	169.7	171.2
13′	–	–	–	53.6

Finally, **2** was a dimeric tetrahydroxanthone as shown in Fig. 1 and was named usneaxanthone B.

Compound **3** was assigned by the molecular formula of $C_{31}H_{30}O_{13}$ by negative HRESIMS analysis ($[M\text{-}H]^-$ *m/z* 609.1607, calcd 609.1608), which was 42 units less than those of **1** and **2**. The comparison of the ^{13}C and ^{1}H NMR spectroscopic data of **1** and **3** (Tables 1 and 2) indicated that the acetoxy group at C-5 in **1** was disappeared in **3**. These data, in conjunction with its molecular formula, suggested that the acetoxy moiety was replaced by a hydroxyl moiety in **3**, confirmed by the corresponding proton at δ_H 3.80 (-CH-OH) and ^{13}C NMR spectra data of **3**.

The comparison ECD method was used to assign axial chirality of compound **3**. The ECD curves of **3** were almost identical to those of **1**, particularly the similar patterns of positive exciton coupling near 215 nm indicated an *aR* axial configuration for compound **3** (Fig. 3), which is in agreement with compound **1**. The absolute configurations in two monomeric units of **3** were proposed to be the same as those in **1**, as indicated by similar NMR data (Table 1), and the coupling constants. Moreover, its absolute configurations were finally deduced as (5*S*,8a*S*,10a*R*,5′*R*,6′*R*,8′*S*,8'a*S*) by X-ray diffraction (CCDC 1854042, Fig. 4) with a Flack parameter of 0.07 (7). Therefore, **3** was a new dimeric tetrahydroxanthone and was named usneaxanthone C (Fig. 5).

Usneaxanthone D (**4**) was obtained as yellow crystals. Its molecular formula was deduced to be $C_{34}H_{32}O_{14}$ (19 DBEs) by HRESIMS (*m/z* 687.1733 $[M + Na]^+$, calcd 687.1690). The ^{1}H NMR spectroscopic data (Table 1) of **4** was similar to those of eumitrin A1 isolated from *Usnea bayleyi* [8], except for the replacement of the hydroxyl group at C-8 in eumitrin A1 by an olefinic proton (δ_H 7.30, H-8) in **4**, which was further supported by correlations of signal at δ_H 7.30 with C-9 (δ_C 184.7), and C-10a (δ_C 80.9) in the HMBC spectrum of **4** (Fig. 6). The configurations of **4** were identical to those of eumitrin A1 by detailed analysis of 1D and 2D NMR spectra of **4**. The similar patterns of positive exciton coupling near 215 nm between **4** and **1** indicated an *aR* axial configuration for **4** (Fig. 3). Additionally, the X-ray diffraction experiment using Cu K_α radiation with Flack parameter of 0.03 (8) confirmed the absolute configurations of **4** to be (5*S*,10a*R*,5′*S*,6′*S*,10'a*R*) (Fig. 6).

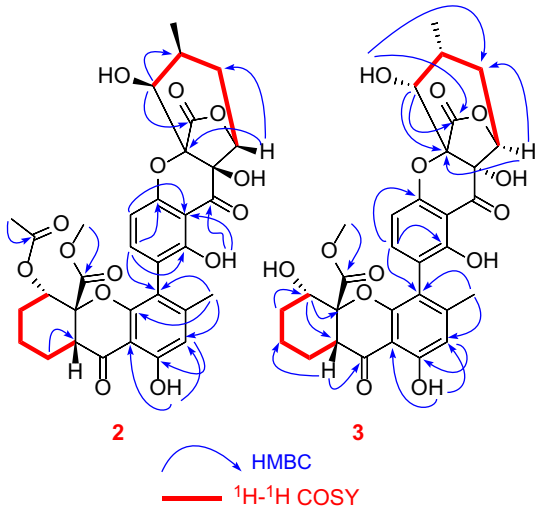

Fig. 5. Key 2D correlations of **2** and **3**.

Several crude extracts and isolated compounds from *Usnea* lichens have been screened against different cancer cell lines showing promising anti-cancer and cytotoxic activities [20,21]. In this work, the isolated compounds **1**, **2** and **4** were evaluated for their *in vitro* cytotoxicity against HT-29 human colorectal cancer cell line using the MTT reduction assay [22], and 5–fluorouracil was used as the positive control (due to amount limitations, **3** was not tested). Compound **4** exhibited potential cytotoxicity against HT–29 cancer cell line with IC_{50} values of 2.41 μM. (Table 3, Fig. 7).

3. Experimental section

3.1. General experimental procedures

Optical rotations were measured on a Kruss digital polarimeter. The UV spectra were recorded on a UV-2550 UV–Vis spectrometer (Shimadzu, Kyoto, Japan). The ECD spectra were measured with a JASCO *J*-815 circular dichroism spectrometer (JASCO, Inc., Tokyo, Japan). The IR spectra were measured on a Nicolet 6700 FT-IR spectrometer. The NMR spectra were recorded on a Bruker 400 AVANCE spectrometer (400 MHz for ^{1}H and 100 MHz for ^{13}C). $CDCl_3$ was used both as a solvent and as an internal reference at δ_H 7.26 and δ_C 77.2, respectively. The HRESIMS data were obtained using a Bruker microOTOF Q-II. The TLC was carried out on precoated silica gel 60 F_{254} and silica gel 60 RP–18 $F_{254}S$ (Merck). Gravity column chromatography was performed with silica gel 60 (0.040–0.063 mm, Silicycle). Size-exclusion chromatography was performed with Sephadex LH-20 (25–100 μm, GE Healthcare). The plates were analyzed under UV light or treated with a solution of 5% vanillin in acidic ethanolic solution followed by heating.

3.2. Lichen material

The thalli of the lichen were separated from the bark of various old trees at 2100–2200 m altitude in Dalat City, Lam Dong province, Vietnam in July – August 2015. The species was authenticated as *Usnea aciculifera* Vain by Dr. Harrie Sipman (Botanic Garden and Boany Museum Berlin – Dahlem, Freie University of Berlin, Germany). A voucher specimen (No US-B029) was deposited at the Herbarium of the Department of Organic Chemistry, University of Science, National

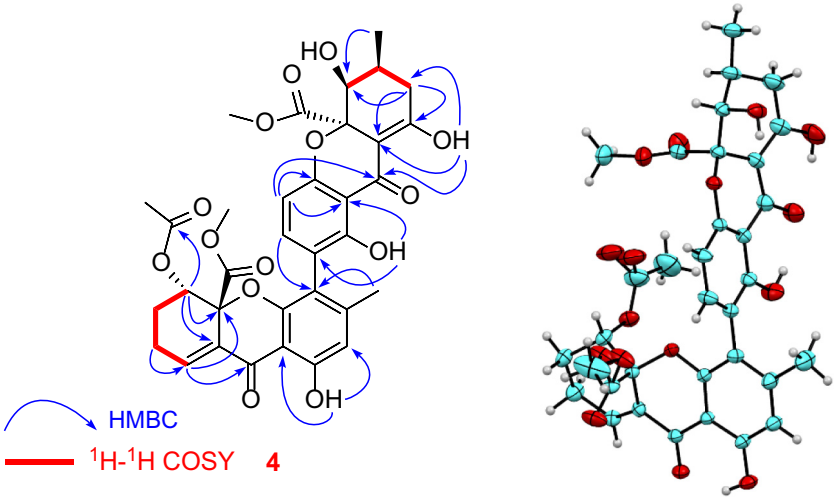

Fig. 6. Key 2D NMR correlations and X-ray structure of **4.**

Table 3
IC_{50} values of **1**, **2**, **4** and 5-fluorouracil on HT-29 colorectal cancer cells[a].

Compound	IC_{50} ± SD
1	> 30
2	> 10
4	2.41 ± 0.33
5-Fluorouracil[b]	> 30

[a] Cytotoxicity was expressed as the mean values of three experiments ± SD; the other isolated compounds were inactive (IC_{50} > 10–30 μM).
[b] 5-Fluorouracil was tested as positive control.

University – Ho Chi Minh City – Vietnam.

3.3. Extraction and isolation

Before extraction, the lichen was carefully inspected for contaminants. Air-dried parts of *U. aciculifera* (2.02 kg) were ground and extracted with *n*-hexane, CH_2Cl_2, EtOAc, and methanol (4 × 10 L), respectively, by the maceration method at ambient temperature, and the filtered solution was evaporated under reduced pressure to afford a *n*-hexane extract (50.0 g), CH_2Cl_2 extract (101.0 g), EtOAc extract (110.0 g) and methanol extract (55.0 g). The CH_2Cl_2 extract was subjected to silica gel column chromatography using gradient elution with *n*-hexane–EtOAc (stepwise 80:20–0:10) and EtOAc–MeOH (stepwise 10:0–0:10) to give thirteen fractions, DCM.1–DCM.13.

Fraction DCM.2 (10.8 g) was subjected to silica gel column chromatography eluted with *n*-hexane–EtOAc (8:2) to give five sub-fractions

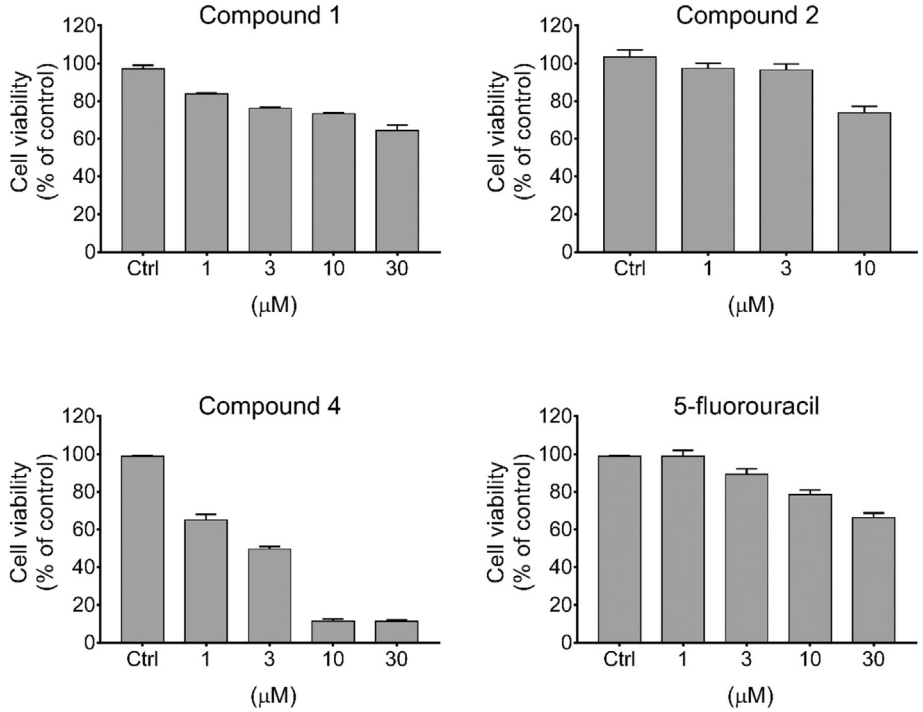

Fig. 7. Cytotoxic activity against HT-29 colorectal cancer cells of **1**, **2**, **4** and 5-fluorouracil.

2.1–2.5. Sub-fraction 2.2 (0.8 g) was chromatographed with RP–C_{18} silica gel eluted with H_2O–MeOH (60:40) to give **2** (4.1 mg), and **3** (3.4 mg). Sub-fraction 2.3 (3.3 g) was purified by a Sephadex LH–20 column (100 g) with MeOH followed by chromatography with RP–C_{18} silica gel eluted with H_2O–MeOH (60:40) to yield **1** (10.8 mg). Sub-fraction 2.4 (4.1 g) was subjected to silica gel column chromatography using gradient elution with *n*-hexane–CH_2Cl_2 (70:30–0:100) to give **4** (5.5 mg).

Usneaxanthone A (**1**). light yellow crystals; $[\alpha]_D^{25} = -232$ (*c* 0.002, MeOH); mp 175 °C; UV (MeOH) λ_{max} (log ε) 238 (2.8), 270 (1.3), 315 (0.8) nm; ECD ($\Delta\varepsilon$) (3×10^{-4} M, MeOH, MeOH) 319 (+5.94), 293 (+0.50), 274 (+8.00), 234 (−21.37), 213 (+15.36); IR (KBr) ν_{max}: 3419, 3377, 1733, 1613, 1309 cm^{-1}; ^1H and ^{13}C NMR ($CDCl_3$) data, see Tables 1 and 2; HRESIMS *m/z* 653.1862 $[M + H]^+$ (calcd for $C_{33}H_{33}O_{14}$, 653.1865) and *m/z* 675.1681 ($[M + Na]^+$, calcd 675.1645). . (Figs. S1-S6, Supporting Information).

Usneaxanthone B (**2**). light yellow crystals; $[\alpha]_D^{25} = +286$ (*c* 0.002, MeOH); mp 176 °C; UV (MeOH) λ_{max} (log ε) 218 (4.2), 235 (4.0), 270 (2.5), 309 (2.4) nm; ECD ($\Delta\varepsilon$) (3×10^{-4} M, MeOH, MeOH) 313 (+2.08), 288 (+14.63), 244 (+6.41), 257 (+4.60), 218 (−39.59); IR (KBr) ν_{max}: 3424, 1733, 1607, 1299 cm^{-1}; ^1H and ^{13}C NMR ($CDCl_3$) data, see Tables 1 and 2; HRESIMS *m/z* 675.1711 $[M + Na]^+$ (calcd for $C_{33}H_{32}O_{14}Na$, 675.1690). (Figs. S7-S12, Supporting Information).

Usneaxanthone C (**3**). colorless needles; $[\alpha]_D^{25} = -238$ (*c* 0.002, MeOH); mp 180 °C; UV (MeOH) λ_{max} (log ε) 220 (4.2) and 330 (1.2) nm; ECD ($\Delta\varepsilon$) (3×10^{-4} M, MeOH) 317 (+6.00), 294 (+2.43), 276 (+14.18), 239 (−39.55), 215 (+26.61); IR (KBr) ν_{max}: 3418, 1725, 1606, 1294 cm^{-1}; ^1H and ^{13}C NMR ($CDCl_3$) data, see Tables 1 and 2; HRESIMS *m/z* 609.1607 $[M-H]^-$ (calcd for $C_{31}H_{29}O_{13}$, 609.1608). (Figs. S13-S18, Supporting Information).

Usneaxanthone D (**4**). light yellow crystals; $[\alpha]_D^{25} = +211$ (*c* 0.002, MeOH); mp 192 °C; UV (MeOH) λ_{max} (log ε) 220 (2.1), 270 (1.0), 310 (0.7) nm; ECD ($\Delta\varepsilon$) (3×10^{-4} M, MeOH) 345 (−0.75), 311 (+3.67), 287 (−1.56), 270 (+3.19), 236 (−26.3), 211 (+29.7); IR (KBr) ν_{max}: 3727, 3631, 1742, 1700, 1606, 1298 cm^{-1}; ^1H and ^{13}C NMR ($CDCl_3$) data, see Tables 1 and 2; HRESIMS *m/z* 687.1733 $[M + Na]^+$ (calcd for $C_{34}H_{32}O_{14}Na$, 687.1690). (Figs. S19-S24, Supporting Information).

3.4. X-ray crystallographic analysis of 1–4

Four compounds crystallize in the following crystal systems, space groups of monoclinic $P2_1$ (**2**, **3**) and orthorhombic $P2_12_12_1$ (**1**, **4**). Colorless or light yellow single crystal with appropriate sizes of each compound was glued on the tip of a MiTeGen microloop. Diffraction data were collected at 296(2) K on a Bruker X8 PROSPECTOR Kappa CCD area-detector diffractometer with an IμS X-ray microfocus source (Cu-Kα radiation, λ = 1.54178 Å), with the help of APEX2 Software Suite [23]. Data were integrated, reduced by SAINT+, corrected for absorption effects and scaled by SADABS, and finally merged by XPREP, implemented in APEX2 Software Suite [23], to yield independent reflections with $R_{int} < 5.0\%$, except those of **4** with $R_{int} = 9.2\%$ (Table S1). The four structures were solved by intrinsic phasing method with SHELXTL XT [24] and refined anisotropically by full matrix least-squares on F^2 with SHELXTL XLMP [25]. The final $R_1(F^2)$ [$F^2 > 2\sigma(F^2)$] values are a bit high in the range of 5.5–7.2% due to the disordered methoxy groups and solvent molecules. The estimated Flack parameters [26] are close to null, indicating the absolute structures of four compounds are reliably determined. Data have been deposited with the Cambridge Crystallographic Data Centre (CCDC nos. 1,854,036–1,854,042). Copies of these data can be obtained, free of charge, on application to the CCDC *via* www.ccdc.cam.ac.uk/conts/retrieving.html (or 12 Union Road, Cambridge CB2 1EZ, UK, fax: +441,223 336,033, e-mail: deposit@ccdc.cam.ac.uk).

3.5. Cell viability assay

HT-29 cells were seeded into 96-well plates at 5×10^3 cells/well. After overnight incubation, cell were treated with compounds **1**, **4** and 5-fluorouracil at concentrations of 1, 3, 10, and 30 μM, compound **2** at concentrations of 1, 3, and 10 μM or 0.2% dimethyl sulfoxide (DMSO; vehicle control) for 48 h. MTT solution was added and incubated for additional 4 h. The medium was removed and 200 μL of DMSO was added to each well. The absorbance of the converted dye was measured at 570 nm using a microplate reading spectrophotometer. IC_{50} values were calculated using GraphPad Prism 7 software.

Acknowledgments

One of us, Truong L. Tuong thanks to Chulalongkorn University – ASEAN Scholarship 2017 and the 90th Anniversary of Chulalongkorn University Scholarship. T. Aree acknowledges the Ratchadaphiseksomphot Endowment Fund, Chulalongkorn University for partial support of X-ray diffraction analysis (CU-58-021-FW). This study was in addition partly supported by Special Task Force for Activating Research Ratchadaphiseksomphot Endowment Fund, grant number GSTAR 59–005–30-001 and the Thailand Research Fund *via* Directed Basic Research Grant (Grant no. DBG6180029).

Conflict of interest

We don't have any conflict of interest.

Appendix A. Supplementary data

Supplementary data to this article can be found online at https://doi.org/10.1016/j.fitote.2019.104194.

References

[1] W. Tim, B. Stefan, S.M. Kye, Xanthone dimers: a compound family which is both common and privileged, Nat. Prot. Rep. 32 (2015) 6–28.
[2] W. Wang, L. Yanyan, H. Xiaomei, T. Chao, C. Peng, A novel xanthone dimer derivative with antibacterial activity isolated from the bark of *Garcinia mangostana*, Nat. Prod. Res. 32 (2018) 1769–1774.
[3] R. Tomáš, S. Karel, Hirtusneanoside, an unsymmetrical dimeric tetrahydroxanthone from the Lichen *Usnea hirta*, J. Nat. Prod. *70* (2007) 1487–1491.
[4] C. Chutrakul, T. Boonruangprapa, R. Suvannakad, M. Isaka, P. Sirithunya, T. Toojinda, K. Kirtikara, Ascherxanthone B from *Aschersonia luteola*, a new antifungal compound active against rice blast pathogen *Magnaporthe grisea*, J. Appl. Microbiol. 107 (2009) 1624–1631.
[5] I. Masahiko, P. Somporn, K. Kanokarn, S. Janya, A cytotoxic xanthone dimer from the Entomopathogenic Fungus *Aschersonia* sp. BCC 8401, J. Nat. Prod. *68* (*2005*) *975–996*.
[6] M. Kye-Simeon, B. Stefan, Xanthones from fungi, lichens, and bacteria: The natural products and their synthesis, Chem. Rev. 112 (2012) 3717–3776.
[7] T. Noriko, T. Hiroshi, M. Keiichi, O. Satoshi, Structure and biosynthesis of xanthoquinodins, Anticoccidal Antibiotics, J. Am. Chem. Soc. 115 (1993) 8558–8564.
[8] D.M. Yang, N. Takeda, Y. Iitaka, V. Sankawa, S. Shibata, Structure of Eumitrin A1, A2 and B. The yellow pigments of the lichen, *Usnea bayleyi (Stirt.)* Zahlbr, Tetrahedron 29 (1973) 519–528.
[9] B. Proksa, D. Uhrin, T. Liptaj, M. Sturdikova, Neosatorin, an ergochrome biosynthesized by neosartorya fishceri, Phytochemistry 48 (1998) 1161–1164.
[10] L. Tian-Xiao, Y. Ming-Hua, W. Ying, W. Xiao-Bing, L. Jun, L. Jian-Guang, K. Ling-Yi, Unusual dimeric tetrahydroxanthone derivatives from *Aspergillus lentulus* and the determination of their axial chiralities, Sci. Rep. 6 (2016) 1–9.
[11] B. Franck, G. Bringmann, G. Flohr, Sequenzanalyse der ergochrom – biosynthese durch konkurrez –incorporation, Angew. Chem. 92 (1980) 483–484.
[12] G. Bringmann, C. Guennther, M. Ochse, O. Schupp, S. Tasler, Biaryl in nature: a multi-facetted class of stereochemically, biosynthetically, and pharmacologically intriguing secondary metabolites, Prog. Chem. Org. Nat. Prod. 82 (2001) 1–249.
[13] S.E. Jamie, B.M.B.M. Nicholas, K.A. Paul, A twist of nature – the significance of atropisomers in biological systems, J. Nat. Pro. Rep. 32 (2015) 1562–1583.
[14] W.M. Melissa, C. Jon, Dicerandrols, New antibiotic and cytotoxic dimers produced by the Fungus *Phomopsis longicolla* isolated from an Endangered Mint, J. Nat. Prod. *64* (*2001*) *1006–1009*.
[15] I. Masahiko, J. Amonlaya, R. Kamolchanok, D. Kannawat, T. Morakot, T. Yodhathai, Phomoxanthones A and B, novel xanthone dimers from the endophytic fungus *Phomopsis* Species, J. Nat. Prod. *64* (*2001*) *1015–1018*.
[16] N. Berova, P.L. Polavarapu, K. Nakanishi, R.W. Woody, Comprehensive chiroptical

spectroscopy: Applications in stereochemical analysis of synthetic compounds, Natural Products, and Biomolecules, 2 John Wiley & Sons, Inc., Hoboken, NJ, USA, 2012.
[17] R. David, D. Abdessamad, M. Attila, V. Vera, B. Philip, S. Björn, E. Laura, H. Alexandra, S. Richard, D. Marc, W. Victor, L. WenHan, K.U. Matthias, J. Christoph, S. Stefanie, W. Sebastian, K. Tibor, A.H. Amal, P. Peter, Pro-apoptotic and immunostimulatory tetrahydroxanthone dimers from the endophytic fungus *Phomopsis longicolla*, J. Org. Chem. 78 (2013) 12409–12412 425..
[18] G. Wu, G. Yu, T. Kurt_an, A. M_andi, J. Peng, X. Mo, M. Liu, H. Li, X. Sun, J. Li, T. Zhu, Q. Gu, D. Li, Versixanthones A-F, cytotoxic xanthone-chromanone dimers from the marine-derived fungus *Aspergillus versicolor* HDN1009, J. Nat. Prod. 78 (2015) 2691–2698.
[19] D.F. Howard, G. Bernardinelli, The use of X-ray crystallography to determine absolute configuration, Chirality 20 (2008) 681–690.
[20] S. Gajendra, C.L.St. Larry, Lichens: a promising source of antibiotic and anticancer drugs, Phytother. Res. 12 (2013) 229–244.
[21] R. Branislav, K. Marijana, S. Tatjana, V. Perica, M. Nedeljko, Biological Activities of *Toninia candida* and *Usnea barbata* together with their norstictic acid and usnic acid constituents, Int. J. Mol. Sci. 13 (2012) 14707–14714 722..
[22] T. L. Riss, R. A. Moravec, A. L. Niles, S. Duellman, H. A. Benink, T. J. Worzella, L. Minor, Cell viability assays. 2013 G. S. Sittampalam, N. P. Coussens, K. Brimacombe, et al., . Eli Lilly & Company and the National Center for Advancing Translational Sciences; 2004. Guidance Manual [Internet]. Bethesda (MD): Eli Lilly & Company and the National Center for Advancing Translational Sciences; 2004.
[23] Bruker, APEX2 v.2014.9-0, Bruker AXS Inc., Madison, WI, 2014.
[24] Bruker, SHELXTL XT, Program for Crystal Structure Solution, v. (2014)/4, Bruker AXS Inc, Madison, WI, 2014.
[25] Bruker, SHELXTL XLMP Program for Crystal Structure Refinement - Multi-CPU, v. 2014/7, Bruker AXS Inc., Madison, WI, 2014.
[26] P. Simon, D.F. Howard, W. Trixie, Use of intensity quotients and differences in absolute structure refinement, Acta Cryst. B69 (2013) 249–259.